Author(s): Kettunen, Henrik & Wallén, Henrik & Sihvola, Ari

Title: Electrostatic resonances of a negative-permittivity hemisphere

Year: 2008

Version: Final published version

Please cite the original version:

Kettunen, Henrik & Wallén, Henrik & Sihvola, Ari. 2008. Electrostatic resonances of a negative-permittivity hemisphere. Journal of Applied Physics. Volume 103, Issue 9. 094112/1-8. 0021-8979 (printed). DOI: 10.1063/1.2917402.

Electrostatic resonances of a negative-permittivity hemisphere

Henrik Kettunen, Henrik Wallén, and Ari Sihvola

Citation: Journal of Applied Physics **103**, 094112 (2008); doi: 10.1063/1.2917402
View online: http://dx.doi.org/10.1063/1.2917402
View Table of Contents: http://scitation.aip.org/content/aip/journal/jap/103/9?ver=pdfcov
Published by the AIP Publishing

Electrostatic resonances of a negative-permittivity hemisphere

Henrik Kettunen,[a] Henrik Wallén, and Ari Sihvola
Department of Radio Science and Engineering, Helsinki University of Technology, P.O. Box 3000, FI-02015 TKK, Finland

(Received 23 November 2007; accepted 4 March 2008; published online 14 May 2008)

This article studies the electric response of an electrically small hemispherical object with negative permittivity by computing its polarizability which is determined by two orthogonal components, the axial one and the transverse one. A certain range of negative permittivity values is found where the mathematical determination of the polarizability becomes impossible due to an unlimited number of singularities. These singularities are due to surface plasmons, also referred to as electrostatic resonances, caused by the sharp edge of the hemisphere. It is also found that the planar surface of the hemisphere may support resonant surface modes. Furthermore, there exists a dipolar resonance determined by the overall geometry. In addition, it is shown that the resonances can be smoothened by introducing losses and, even more importantly, rounding the edge. © *2008 American Institute of Physics*. [DOI: 10.1063/1.2917402]

I. INTRODUCTION

This article focuses on explaining the resonant behavior of the electric response of a small dielectric hemisphere which is observed when computing its polarizability with negative permittivity ϵ. Objects with negative permittivity are capable of supporting surface plasmons or electrostatic resonance modes,[1,2] and, in this article, these resonant modes are studied for a hemispherical geometry using an electrostatic approach. Similar behavior can also be observed for the magnetic response if the permeability μ of the object becomes negative. Negative material parameters have recently become an object of major interest. One reason for this is the possibility of realizing these negative parameters by means of artificial metamaterials.[3]

In a uniform external electric field, a dielectric object becomes polarized. In the far field, the polarized object can be approximated as an electric dipole because the higher order field components decay quickly as a function of distance. The polarizability of the object α_{abs} is determined as the ratio of the induced dipole moment $\mathbf{p}$ and the external electric field $\mathbf{E}_e$,

$$\mathbf{p} = \alpha_{\text{abs}} \mathbf{E}_e. \tag{1}$$

The polarizability can be determined by first solving the electrostatic potential functions inside and outside the object. Polarizability is clearly an electrostatic concept. However, negative values of permittivity are possible only in the frequency domain. Therefore, the object must be assumed very small with respect to the wavelength of the external electromagnetic field. In this quasistatic situation, the potential must satisfy the Laplace equation.

It is often more convenient to present the polarizability as a dimensionless number, normalized by the volume of the object and the permittivity of the environment $\alpha = \alpha_{\text{abs}}/(V\epsilon_e)$. For example, the normalized polarizability of a homogeneous sphere has a simple analytical expression

$$\alpha = 3\frac{\epsilon_r - 1}{\epsilon_r + 2}, \tag{2}$$

where the relative permittivity ϵ_r is the permittivity contrast between the object and the environment. If $\epsilon_r = -2$, the polarizability tends to infinity. In this article, these singularities and the corresponding permittivity values are studied in the case of a hemispherical object.

When considering the polarizability of a homogeneous sphere, only one singularity is found which is due to a static dipolar resonance. Instead, for the hemisphere, an unlimited number of singularities occur within a certain permittivity range. This is caused by the sharp edge of the hemisphere which locally forms a 90° wedge.[4] Secondly, it is known that an interface between media with permittivities of opposite numbers is capable of supporting surface plasmons.[5] This applies to the flat surface of the hemisphere when $\epsilon_r = -1$. In addition, dipolar resonances are found. Their occurrence is dependent on the direction of the external field.

We begin by introducing a semianalytical method for computing the polarizability components for a hemispherical object and present the obtained results for negative permittivities. We continue by explaining the singularities of the results and studying analytical expressions for the resonant modes in cases of the 90° wedge and the planar surface. We also discuss the dipolar resonance, which, in the case of transverse excitation, can be traced quite accurately by matrix eigenvalue analysis. Finally, we consider the effect of losses and numerically test the rounding of the edge.

Some results of this study were presented in two conference presentations at Metamaterials'2007.[6,7]

II. COMPUTATION OF THE POLARIZABILITY COMPONENTS

For the hemisphere, expression (1) must be written in a more general form

[a]Electronic mail: henrik.kettunen@tkk.fi.

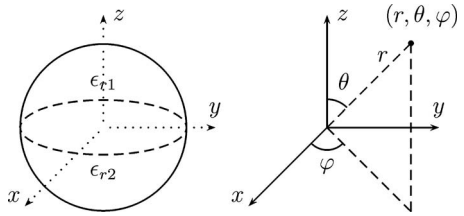

FIG. 1. Double hemisphere located in the spherical coordinate system.

$$\mathbf{p} = \bar{\bar{\alpha}}_{\text{abs}} \cdot \mathbf{E}_e, \tag{3}$$

where the polarizability is expressed as a dyadic. The normalized polarizability can be written as

$$\bar{\bar{\alpha}} = \alpha_t(\mathbf{u}_x\mathbf{u}_x + \mathbf{u}_y\mathbf{u}_y) + \alpha_z\mathbf{u}_z\mathbf{u}_z. \tag{4}$$

It is determined by two orthogonal components: the axial and the transverse polarizabilities, α_z and α_t, respectively. These components can be solved separately by using two orthogonal external fields with unit magnitude, one parallel and one transverse to the rotational axis of the hemisphere which is now chosen to be the z axis, that is, in the axial case the external field is z directed and in the transversal case the field is chosen x directed. Our previous article[8] considers a method for computing these components and all required formulas can be found therein. In this article, the procedure is explained very briefly.

The polarizabilities can be solved by considering the hemisphere as a special case of a so-called double hemisphere (see Fig. 1) which is a sphere with unit radius consisting of two equally large hemispheres with different permittivities, that is, the space is divided into three regions.

The potential function must satisfy the Laplace equation, $\nabla^2\phi(r,\theta,\varphi)=0$, in all three regions. The solutions are written as series expansions and the unknown coefficients are solved by applying the boundary conditions. The continuities of the potential and the normal component of the electric displacement are required on every interface between the regions.

When computing the polarizabilities, only the coefficients in the region outside the double hemisphere are needed, but since there is no closed-form solution, this requires constructing and solving an infinite equation system where each equation includes an infinite sum. In order to achieve numerical results in practice, N equations are taken each consisting a truncated sum over N terms and the equation system is written as an $N\times N$ matrix equation

$$\mathbf{MB} = \mathbf{A}, \tag{5}$$

where $\mathbf{B}$ is a vector consisting of the desired coefficients.

In the case of the axial polarizability α_z,

$$M_{ln} = [\eta_l(n+1) + \eta_l l\epsilon_{r1} + (-1)^{n+l}(n+1) + (-1)^{n+l}l\epsilon_{r2}]U_{n,l} \tag{6}$$

and

$$A_l = [\eta_l l\epsilon_{r1} - \eta_l + (-1)^{1+l}l\epsilon_{r2} - (-1)^{1+l}]U_{1,l}, \tag{7}$$

where

$$\eta_l = \begin{cases} \frac{\epsilon_{r2}}{\epsilon_{r1}}, & l \text{ odd}, \\ 1, & l \text{ even} \end{cases} \tag{8}$$

and

$$U_{n,l} = \int_0^1 P_n(\xi)P_l(\xi)d\xi, \tag{9}$$

where $P_n(\xi)$ are the Legendre polynomials[9] of the order n. The analytical expressions for the integrals (9) are presented in Ref. 8.

In the case of transverse polarizability α_t, the matrix elements become

$$M_{ln} = [\eta_l(n+1) + \eta_l l\epsilon_{r1} + (-1)^{n+l}(n+1) + (-1)^{n+l}l\epsilon_{r2}]U^1_{n,l} \tag{10}$$

and

$$A_l = [\eta_l l\epsilon_{r1} - \eta_l + (-1)^{1+l}l\epsilon_{r2} - (-1)^{1+l}]U^1_{1,l}, \tag{11}$$

where

$$\eta_l = \begin{cases} 1, & l \text{ odd}, \\ \frac{\epsilon_{r2}}{\epsilon_{r1}}, & l \text{ even} \end{cases} \tag{12}$$

and

$$U^1_{n,l} = \int_0^1 P^1_n(\xi)P^1_l(\xi)d\xi, \tag{13}$$

where $P^1_n(\xi)$ are the associated Legendre functions.[9] We have, however, omitted the factor $(-1)^m$. The integrals (13) are also analytically evaluable.[8]

The coefficient B_0 can be included in the equation system (5) in the axial case, as in Ref. 8, but it turns out that $B_0=0$ independently of the other coefficients B_n. Therefore, in both cases, the indices n and l run from 1 to N.

The polarizability of the object is determined by the dipolar term of the series expansion of the potential outside the object. The normalized polarizabilities for the double hemisphere become

$$\alpha = 3B_1. \tag{14}$$

A single hemisphere is obtained by choosing the permittivity of the other half equal to the permittivity of the environment, that is $\epsilon_{r2}=1$. It must be noticed that the polarizability of a single hemisphere must be normalized by a volume half of the volume of the double hemisphere. Therefore, for the hemisphere

$$\alpha = 6B_1. \tag{15}$$

For the normalized axial polarizability α_z, B_1 is solved from Eq. (5) using Eqs. (6) and (7) and for the normalized transverse polarizability α_t, B_1 is solved using Eqs. (10) and (11).

III. COMPUTATIONAL RESULTS FOR THE POLARIZABILITIES

Let us present computational results for the polarizabilities. As documented,[8] with positive permittivities with $N>200$, the presented method gives the accuracy of the or-

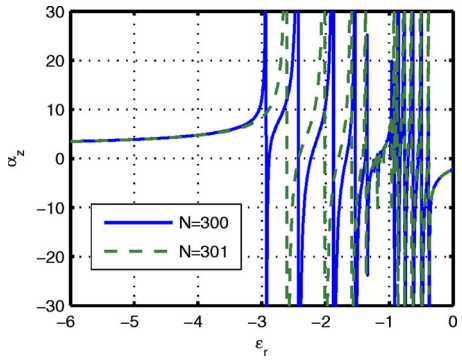

FIG. 2. (Color online) The normalized axial polarizability α_z as a function of the relative permittivity ϵ_r.

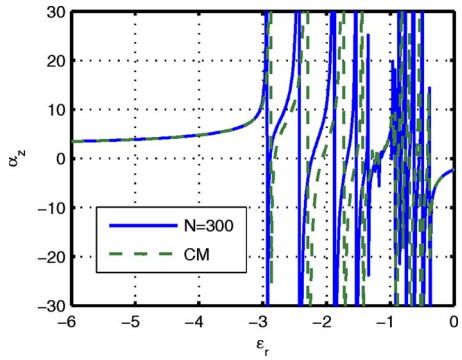

FIG. 4. (Color online) The normalized axial polarizability compared with the result computed using CM.

der of 10^{-5}. When applied for negative permittivities, the same accuracy is achieved with $N>400$ with $\epsilon_r<-10$. In other words, the method works nicely for permittivities negative enough. However, there exists a certain permittivity range where this method fails to produce reasonable results.

In Figs. 2 and 3, the polarizabilities α_z and α_t are plotted as functions of ϵ_r computed with different matrix sizes N. The actual polarizability values cannot be read from these figures. They are only showing that in both cases there is a permittivity range where there are several singularities and the solution does not converge. The matrix size N corresponds to N singularities, that is, their number is unlimited. For both polarizability components, the problematic region is between $-3<\epsilon_r<-1/3$. Moreover, this region divides into two subregions, as the singularities seem to stabilize near $\epsilon_r=-1$. Also, in the transverse case, there is a quite stable singularity near $\epsilon_r=-4$.

In Fig. 4 the normalized axial polarizability with $N=300$ is compared with the result computed numerically using COMSOL MULTIPHYSICS 3.3 (CM) which is a commercial software based on finite element method. With CM, the rotational symmetry of the hemisphere can be utilized. That is, with both the axial and the transverse excitation, the geometry can be modeled in two dimensions. In computation of the curve presented in Fig. 4, a dense mesh consuming 225 217 degrees of freedom is used. However, within the permittivity range $-3<\epsilon_r<-1/3$ the solution does not converge and the result is highly dependent on the discretization. Again, with permittivities negative enough, the results coincide very well.

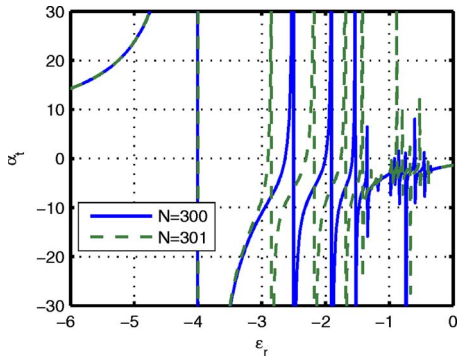

FIG. 3. (Color online) The normalized transverse polarizability α_t.

The convergence of the solution as a function of N in the axial case with certain permittivity values is plotted in Figs. 5 and 6. Within the problematic range, the result keeps oscillating between the positive and the negative infinity. Outside the range, the method is working again, even though the permittivity is negative.

IV. ELECTROSTATIC RESONANCES CAUSED BY THE EDGE

It is obvious that the sharp edge has its effect on the electric response of the hemisphere. Wedges with negative material parameters and negligible losses are found supporting field modes which oscillate with infinite spatial frequency causing problems with numerical computations.[10] A very crucial thing to notice is that these modes may become unphysically singular, that is, the field energy near the wedge becomes infinite.[11,12]

The radius of curvature of the edge is very large compared with its sharpness and therefore, in close vicinity to the edge, the edge can be considered straight. The effect of the edge can be studied analytically by considering a 90° wedge in cylindrical coordinates. The problem can be divided into two orthogonal situations, the symmetric/even one and the antisymmetric/odd one where the symmetry is defined as a symmetry of the electrostatic potential function with respect to the xz plane (see Fig. 7). An arbitrary uniform external electric field can be given as a superposition of these corresponding even and odd field components.

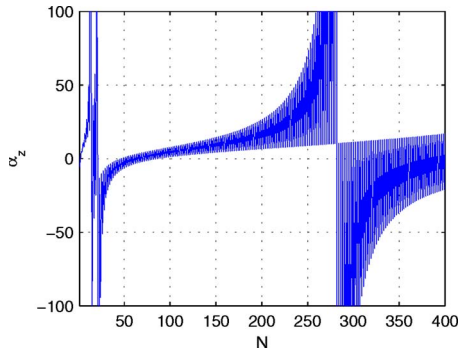

FIG. 5. (Color online) The convergence of the result in the axial case with $\epsilon_r=-2$.

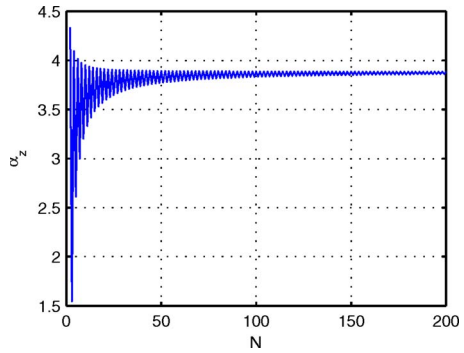

FIG. 6. (Color online) The convergence of the result in the axial case with $\epsilon_r=-5$.

Again, the electrostatic potential function must satisfy the Laplace equation $\nabla^2\phi(\rho,\varphi,z)=0$. In the even case, possible solutions, which also satisfy the continuity of the potential at $\varphi=\varphi_0$, can be written in the form[4]

$$\phi=\begin{cases} K_{j\nu}(q\rho)\dfrac{\cosh(\nu\varphi)}{\cosh(\nu\varphi_0)}\cos(qz), & |\varphi|\le\varphi_0, \\ K_{j\nu}(q\rho)\dfrac{\cosh[\nu(\pi-\varphi)]}{\cosh[\nu(\pi-\varphi_0)]}\cos(qz), & \varphi_0\le\varphi\le 2\pi-\varphi_0, \end{cases} \tag{16}$$

where $K_{j\nu}(q\rho)$ is the modified Bessel function of the second kind with purely imaginary order, that is $\nu>0$ is real. $K_{j\nu}(x)$ has an integral representation[9]

$$K_{j\nu}(x)=\int_0^\infty e^{-x\cosh t}\cos\nu t\,dt \tag{17}$$

and for ν real and x real and positive, it is real valued.

The solutions (16) correspond to the electrostatic edge modes. They decay away from the interface, but they oscillate along it. Moreover, when $\rho\to 0$, $K_{j\nu}(q\rho)$ oscillates with constant amplitude but with increasing spatial frequency. Also, $q>0$ remains an arbitrary constant.

The situation $q=0$ is possible, as well. However, the expressions (16) must be slightly modified. The Bessel function $K_{j\nu}(q\rho)$ is then replaced by $\cos(\nu\ln\rho)$ which behaves similarly when $\rho\to 0$.

The parameter ν can be solved from the relation

$$\epsilon_r=-\frac{\tanh[\nu(\pi-\varphi_0)]}{\tanh(\nu\varphi_0)}. \tag{18}$$

For lossless material, Eq. (18) states that the even resonant modes (16) are possible solutions only for permittivities $-(\pi-\varphi_0)/\varphi_0<\epsilon_r<-1$. In the case of a 90° wedge, that is

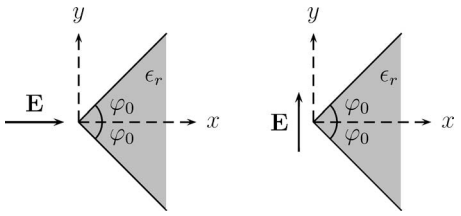

FIG. 7. A dielectric wedge in a symmetric/even case (left) and in an antisymmetric/odd case (right).

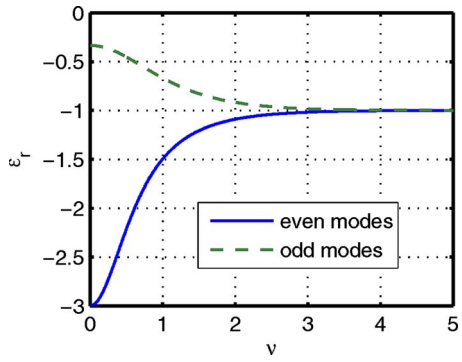

FIG. 8. (Color online) Relation between the relative permittivity ϵ_r and the parameter ν for even and odd edge modes in the case of a 90° wedge plotted using Eqs. (18) and (20), respectively.

$\varphi_0=\pi/4$, this corresponds to the permittivity range $-3<\epsilon_r<-1$.

In the odd case, the potential can be written

$$\phi=\begin{cases} K_{j\nu}(q\rho)\dfrac{\sinh(\nu\varphi)}{\sinh(\nu\varphi_0)}\cos(qz), & |\varphi|\le\varphi_0, \\ K_{j\nu}(q\rho)\dfrac{\sinh[\nu(\pi-\varphi)]}{\sinh[\nu(\pi-\varphi_0)]}\cos(qz), & \varphi_0\le\varphi\le 2\pi-\varphi_0 \end{cases} \tag{19}$$

and, correspondingly, we get

$$\epsilon_r=-\frac{\tanh(\nu\varphi_0)}{\tanh[\nu(\pi-\varphi_0)]}. \tag{20}$$

This implies that the odd resonant modes (19) occur with permittivities $-1<\epsilon_r<-\varphi_0/(\pi-\varphi_0)$. For $\varphi_0=\pi/4$, the range becomes $-1<\epsilon_r<-1/3$. Figure 8 presents the relations (18) and (20) as a function of parameter ν.

When studying the polarizability components of the hemisphere, both even and odd field components are present in both axial and transverse situations. Therefore, the effect of the edge explains the difficulty in determining the polarizabilities α_z and α_t within permittivity range $-3<\epsilon_r<-1/3$, $\epsilon_r\neq-1$.

Figures 9 and 10 present the potential distributions of the hemisphere in xz plane in the vicinity of the edge with external axial electric field. The even and the odd edge modes are recognizable. However, the presented numerical values for the potential are not reliable due to the nonconvergence of the results with the corresponding permittivities.

V. ELECTROSTATIC RESONANCES CAUSED BY THE PLANAR SURFACE

By studying the relations (18) and (20) it can be seen that if the wedge becomes sharper, that is, the angle φ becomes smaller, the permittivity range of the edge modes becomes wider and, vice versa, the increase of the angle φ makes the range narrower. Let us consider the limiting case $\varphi=\pi/2$ which means that the wedge becomes a planar surface. Substitutions into both Eqs. (18) and (20) result in the permittivity value $\epsilon_r=-1$. This suggests that the relative permittivity of negative unity may be significant considering the flat surface of the hemisphere.

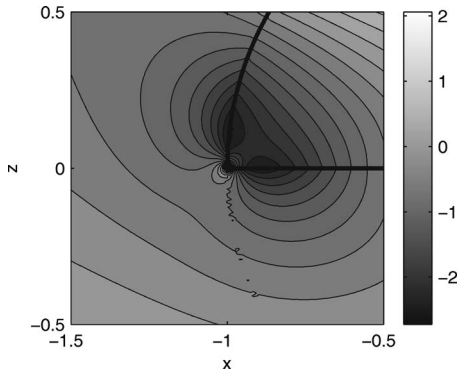

FIG. 9. An even edge mode is visible in the electrostatic potential distribution (ϕ in V) in the xz plane at the edge of the hemisphere with $\epsilon_r=-2$ in a uniform z-directed external electric field.

However, the determination of the polarization components with $\epsilon_r=-1$ seems possible and surprisingly, even though the system matrices (6) and (10) become badly singular, exact numerical values $\alpha_z=6$ and $\alpha_t=-3$ are obtained. We also notice, that B_1 becomes the only nonzero coefficient, that is, the response of the hemisphere is purely dipolar. This indicates that the potential outside the (double) hemisphere can be given in a closed form.[13]

The same thing applies for a double hemisphere with permittivities with opposite signs, that is $\epsilon_{r2}=-\epsilon_{r1}$ (see Fig. 1). In this case, one should note that, as $\epsilon_{r2}\neq 1$, the absolute values of the polarizability must be normalized by the volume of a whole sphere. The polarizability components become independent of the actual value of the permittivity and they seem to have accurate numerical values, $\alpha_z=3$ and $\alpha_t=-3/2$, which give the average polarizability $\alpha_{av}=(\alpha_z+2\alpha_t)/3=0$. Moreover, these values coincide exactly with the polarizabilities of a homogeneous sphere (2) with permittivities $\epsilon_r\to\infty$ (perfect electric conductor) and $\epsilon_r=0$ (perfect magnetic conductor), respectively. This is in very good agreement with Ref. 13.

Furthermore, it is shown in Ref. 13, that if the potential is exceptionally allowed to have a singularity of r^{-2} at the origin, also the potential inside the (double) hemisphere has a closed-form solution. Our semianalytical method[8] does not allow this singularity, and we do not obtain an unambiguous convergent solution for the potential inside the hemisphere.

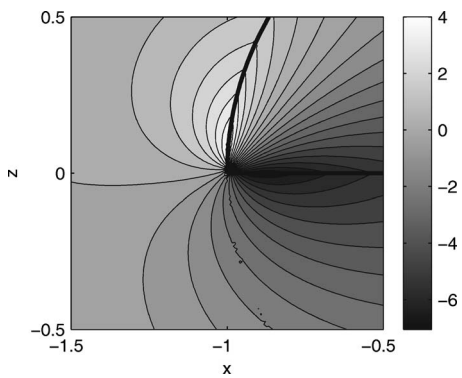

FIG. 10. An odd edge mode is visible in the electrostatic potential distribution (ϕ in V) in the xz plane at the edge of the hemisphere with $\epsilon_r=-1/2$ in a uniform z-directed external electric field.

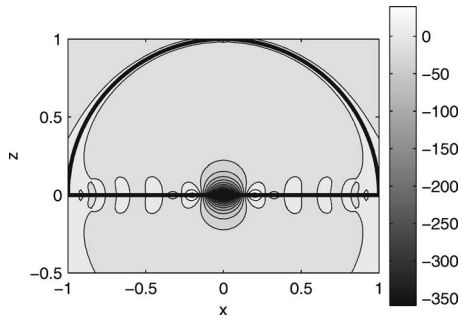

FIG. 11. The electrostatic potential distribution (ϕ in V) of the hemisphere in the xz plane with $\epsilon_r=-1$ in a uniform z-directed external electric field. A surface mode is concentrated on the planar surface.

Figures 11 and 12, presenting the potential distributions, show how strongly oscillating plasmons are concentrated on the planar surface. Similar surface resonances are also present in the numerical results obtained using COMSOL MULTIPHYSICS. In this case, CM fails to find a numerically stable convergent solution.

The reason for the nonuniqueness of the solution can be explained analytically. Locally, especially near the origin, the planar surface of the hemisphere can be approximated by a halfspace. Let the xy plane be the interface between permittivities ϵ_1 and ϵ_2 and let us denote $\epsilon_r=\epsilon_2/\epsilon_1$. Then, for the Laplace equation, a solution which exponentially decays away from the interface is sought. A possible oscillating solution is found in the cylindrical coordinates, that is

$$\phi(\rho,\varphi,z)=\begin{cases} J_n(s\rho)\cos(n\varphi)e^{-sz}, & z\geq 0, \\ J_n(s\rho)\cos(n\varphi)e^{sz}, & z\leq 0, \end{cases} \tag{21}$$

where $s>0$ and n is a non-negative integer. This solution is a local one, as it decays away from the interface but also away from the z axis.

By considering the boundary conditions at $z=0$, in Eq. (21), it can be seen that the resonant surface mode occurs only if $\epsilon_r=-1$. Such interface is also introduced in the context of a perfect lens.[14] The surface modes are evidently related to the amplification of evanescent modes in the lens.

In the case of the hemisphere, these modes are totally localized on the surface and cannot be seen from outside the (double) hemisphere. As noticed earlier, the ambiguity of the solution inside the hemisphere does not affect the polarizability values.

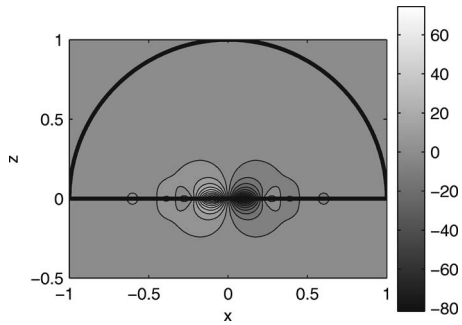

FIG. 12. The electrostatic potential distribution (ϕ in V) of the hemisphere in the xz plane with $\epsilon_r=-1$ in a uniform x-directed external electric field. Again, an excited surface mode is visible.

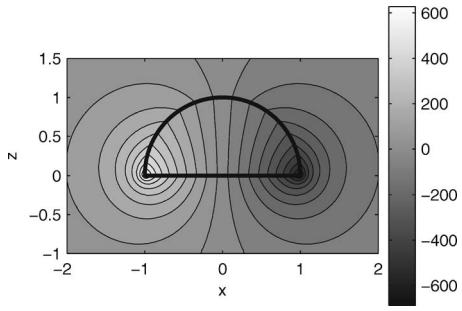

FIG. 13. The electrostatic potential distribution (ϕ in V) of the hemisphere in the xz plane with $\epsilon_r=-4$ in a uniform x-directed external electric field. The response of the hemisphere resembles the one of an electric dipole.

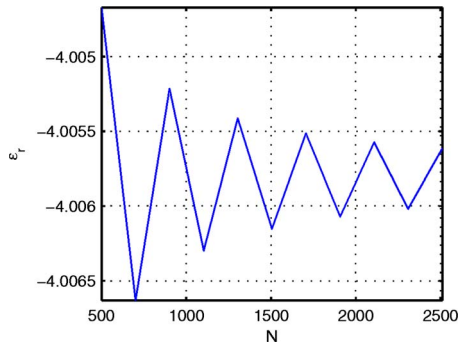

FIG. 14. (Color online) The behavior of the smallest eigenvalue of the system matrix in the transverse case as a function of the matrix size N.

VI. DIPOLAR RESONANCES

However, the edge or surface modes do not explain the singularity of the transverse polarizability at $\epsilon_r \approx -4$ (see Fig. 3). Its stability and the potential distribution (see Fig. 13) indicate that this resonance is of a dipolar nature. As mentioned before, the singularity of the polarizability of a homogeneous sphere (2) is caused by a static dipolar resonance. As a generalization of the sphere, also ellipsoids are geometries whose polarizability components are analytically evaluable.[15] A feasible analytical reference for the hemisphere is, for example, an oblate spheroid with semiaxes chosen as $a_x=a_y=2a_z$. If the radius of the hemisphere is also a_x, the maximum dimensions in the axial and transverse directions for both objects are equal. Also, the objects have the same volume. The singularity of the transverse polarizability of such a spheroid occurs at $\epsilon_r \approx -3.23$ which is outside the range $-3<\epsilon_r<-1/3$. For the hemisphere, the sharp edge seems to shift the corresponding resonance to $\epsilon_r \approx -4$. The shifting of the resonance is clearly seen later when the rounding of the edge is discussed.

The occurrence of the dipolar resonance in the transverse case can actually be determined quite accurately by writing the matrix Eq. (5) as a generalized eigenvalue equation using system matrix (10) and zero excitation as follows:

$$\mathrm{M}_1\mathbf{B} = \epsilon_r \mathrm{M}_2\mathbf{B}, \tag{22}$$

where

$$M_{1\,ln} = m_{1\,ln} U^1_{n,l}, \tag{23}$$

where

$$m_{1\,ln} = \begin{cases} [1+(-1)^{n+l}](n+l)+(-1)^{n+l}l, & l \text{ odd}, \\ (n+1), & l \text{ even} \end{cases}, \tag{24}$$

and

$$M_{2\,ln} = -m_{2\,ln} U^1_{n,l}, \tag{25}$$

where

$$m_{2\,ln} = \begin{cases} l, & l \text{ odd}, \\ [1+(-1)^{n+l}]l+(-1)^{n+l}(n+1), & l \text{ even}. \end{cases} \tag{26}$$

The dipolar resonance at $\epsilon_r \approx -4$ is the smallest eigenvalue which is found and it is much more stable than any other. The corresponding permittivity can be traced with accuracy of four digits. From Fig. 14 it can be seen that the resonance occurs at $\epsilon_r \approx -4.006$.

In the axial case, no dipolar resonance can clearly be observed. The singularity of the axial polarizability of the oblate spheroid occurs at $\epsilon_r \approx -0.897$ and, unfortunately, in the case of the hemisphere, this falls into the permittivity range where the singularities due to the edge dominate the electric response and therefore, the corresponding permittivity value cannot be determined. Even the eigenvalue analysis is of no help.

However, by studying the polarizability curve in Fig. 2, we notice that the in the permittivity range $-1<\epsilon_r<-1/3$ there is a cluster of singularities which looks very strong. The corresponding cluster looks very different in the transverse case (see Fig. 3). This also indicates that, in the axial case, the dipolar resonance occurs somewhere between $-1<\epsilon_r<-1/3$, but it is obscured by the odd edge modes.

VII. EFFECTS OF LOSSES AND ROUNDING OF THE EDGE

So far, we have considered a lossless hemisphere with purely real negative permittivity and with infinitely sharp edge. Let us next study how the addition of losses or rounding of the edge affects the singular response of the hemisphere.

The principle of causality states that it is impossible to achieve negative permittivity values without any losses. In

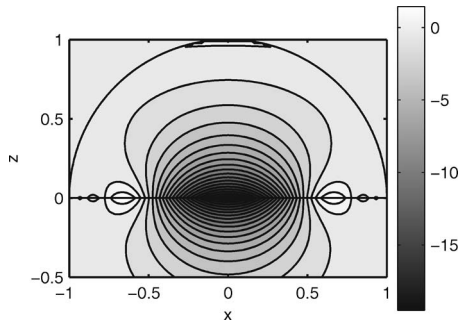

FIG. 15. The electrostatic potential distribution (ϕ in V) of the hemisphere in the xz plane with $\epsilon_r=-1-0.001j$ in a uniform z-directed external electric field. Very small losses can already be seen making the surface modes notably smoother and the solution convergent.

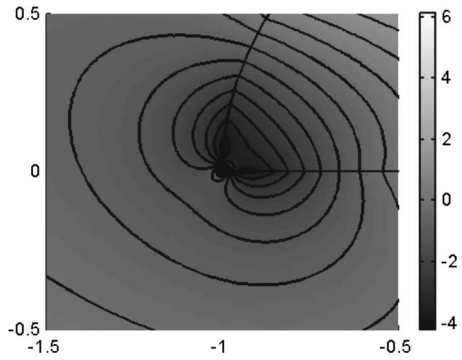

FIG. 16. The electrostatic potential distribution (ϕ in V) of the hemisphere in the xz plane with $\epsilon_r=-2$ in a uniform z-directed external electric field computed using CM. The resonant edge modes are causing problems with the convergence.

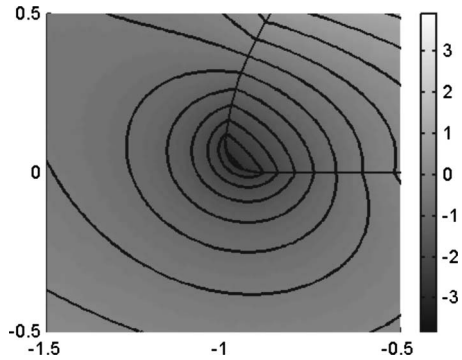

FIG. 18. The electrostatic potential distribution (ϕ in V) of the hemisphere in the xz plane with $\epsilon_r=-2-0.1j$ and with a rounded edge in a uniform z-directed external electric field computed using CM. By the combination of rounding and losses, the solution becomes smooth and the amplitude is attenuated.

real materials, these losses damp the unphysically strong responses. In this quasistatic situation, we introduce losses by writing the permittivity as $\epsilon_r=\epsilon_r'-j\epsilon_r''$.

It turns out that the losses have to be considerably large before they seem to improve the convergence of the result. This is due to the resonant edge modes which are almost unaffected by small losses. Our numerical results, not presented in this article, indicate that with $\epsilon_r'' \geq 0.01\epsilon_r'$, the singularities start to smoothen but for the convergence of the result, ϵ_r' and ϵ_r'' must be equal in magnitude.

On the other hand, the surface modes are smoothened effectively. Figure 15 presents the potential distribution on the planar surface with $\epsilon_r'=-1$ and $\epsilon_r''=0.001$. When compared with the lossless case (see Fig. 11), the effect of small losses is already remarkable. This is also in good agreement with the observation that very small deviations from $\epsilon_r'=-1$, $\epsilon_r''=0$ can severely limit the performance of the perfect lens.[16–18]

Rounding of the edge, instead, offers a practical way to stabilize the unphysically singular edge modes.[11] The semianalytical method presented in Sec. II does not apply anymore for the rounded hemisphere but the effect of rounding can easily be tested numerically using COMSOL MULTIPHYSICS. Figure 16 presents the potential distribution near the sharp edge with $\epsilon_r=-2$. The edge modes prevent the convergence of the result and the situation is the same as in Fig. 9. Figure 17 presents the same edge with a small rounding. It can be seen that near the rounded edge, the potential already behaves much smoother and the solution is more stable. However, the radius of curvature of the edge is still very small and in the lossless case, the potential may still be singular. Figure 18 presents the potential distribution of the same rounded edge but with complex permittivity $\epsilon_r=-2-0.1j$. The losses are clearly damping the magnitude of the response.

Figure 19 presents the transverse polarizability of the hemisphere compared with numerical results computed with two different roundings. First, the sharp edge of the hemisphere is cut and replaced by a circular corner so that the remaining object has 99% of the volume of the original hemisphere. Another larger rounding is preserving 95% of the original volume. From Fig. 19, it can be seen that in the lossless case the rounding does not eliminate the singularities but it makes the range of their occurrence narrower. The dipolar resonance is clearly moving closer to the one of the aforementioned oblate spheroid at $\epsilon_r \approx -3.23$. The most important effect of the rounding is that it makes the spectrum of the singularities discrete. The number of the singularities becomes finite and their places become stable.

Figures 20 and 21 present the effect of the combination of the rounding and the losses on the axial and the transverse polarizabilities, respectively. The edge of the hemisphere is rounded by cutting 1% of the original volume and the rela-

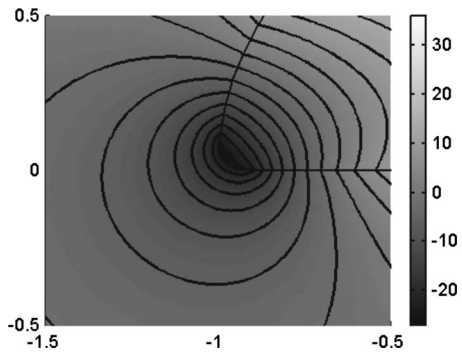

FIG. 17. The electrostatic potential distribution (ϕ in V) of the hemisphere in the xz plane with $\epsilon_r=-2$ and with a rounded edge in a uniform z-directed external electric field computed using CM. The small rounding makes the edge modes notably smoother and improves the convergence.

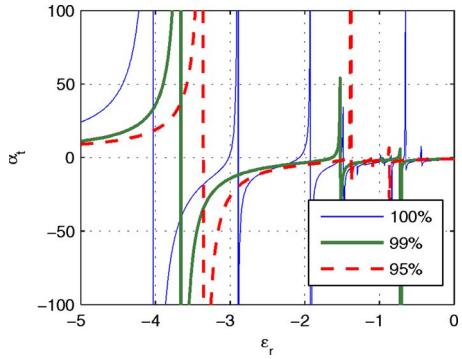

FIG. 19. (Color online) The effect of rouding of the edge in the transverse case. The percentages refer to the volume proportion of the rounded and the original hemisphere.

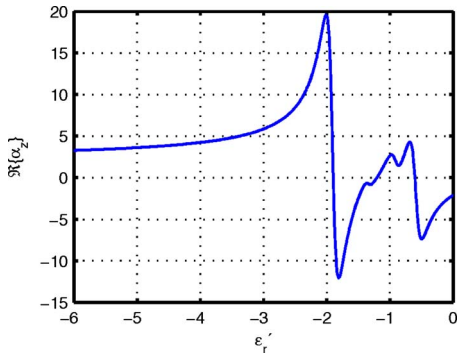

FIG. 20. (Color online) The real part of the normalized axial polarizability of a hemisphere with a rounding of 1% by volume as a function of ϵ_r' with $\epsilon_r''=0.1$.

tive permittivity is given as $\epsilon_r=\epsilon_r'-j\epsilon_j''$ with constant imaginary part $\epsilon_r''=0.1$ The real parts of the polarizabilities are plotted as functions of the real part of the permittivity. The singularities are smoothened and the results are converging nicely. However, notable resonances are still occurring and the polarizabilities have very large values. The most distinguishable resonance is the dipolar one in the transverse case near $\epsilon_r'=-4$ (see Fig. 21). Instead, the axial dipolar resonance between $-1<\epsilon_r'<-1/3$ is effectively attenuated by the losses. The strongest resonance near $\epsilon_r'=-2$ in Fig. 20 cannot be the dipolar one since it is outside the supposed range. It can also be verified from the potential distribution presented in Fig. 18 that the corresponding singularity is caused by the edge. On the whole, the axial response is weaker than the transverse one, which is due to the fact that with axial excitation, all the resonances occur within the range where, with $\epsilon_r''=0.1$, the ratio ϵ_r''/ϵ_r' is relatively large.

VIII. CONCLUSION

The electrostatic response of a hemisphere with negative permittivity was studied by computing its polarizability components. The polarizabilities were found to have an unlimited number of singularities due to electrostatic resonances which were caused by the sharp edge of the hemisphere. The edge was found to support even resonant edge modes with permittivities $-3<\epsilon_r<-1$ and odd edge modes with $-1<\epsilon_r<-1/3$. With $\epsilon_r=-1$, the planar surface supported nonunique resonant surface modes which, however, did not affect the potential outside the (double) hemisphere. Also, in the case of transverse excitation, a dipolar resonance was found at $\epsilon_r\approx-4.006$. In the case of axial excitation, the dipolar resonance was obscured by the odd edge resonances.

By introducing losses, the surface modes were attenuated making the solution convergent near $\epsilon_r=-1$. However, small losses did not notably affect the edge modes. Instead, already a small rounding of the geometry made the edge modes stable. Therefore, the rounding of sharp edges is essential in modeling objects with negative permittivities at which electrostatic resonances may occur. The rounding also narrows the permittivity range of the resonances. In order to achieve convergent results in numerical simulations with all permittivities, both losses and rounding are required.

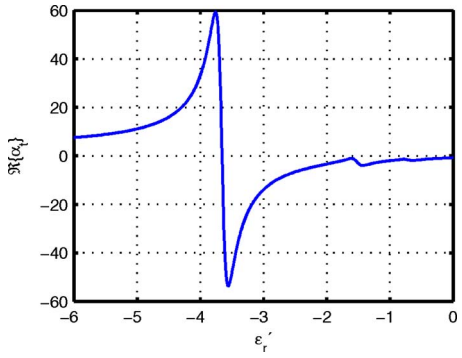

FIG. 21. (Color online) The real part of the normalized transverse polarizability of a hemisphere with a rounding of 1% by volume as a function of ϵ_r' with $\epsilon_r''=0.1$.

ACKNOWLEDGMENTS

This study was supported by the Academy of Finland. The authors would also like to thank Dr. Andrea Alù for fruitful and interesting discussions considering the double hemisphere with opposite permittivities.

[1] C. F. Bohren and D. R. Huffman, *Absorption and Scattering of Light by Small Particles* (Wiley, New York, 1998).
[2] D. R. Fredkin and I. D. Mayergoyz, Phys. Rev. Lett. **91**, 253902 (2003).
[3] M. Lapine and S. Tretyakov, IET Proc. Microwaves, Antennas Propag. **1**, 3 (2007).
[4] L. Dobrzynski and A. A. Maradudin, Phys. Rev. B **6**, 3810 (1972).
[5] E. A. Stern and R. A. Ferrell, Phys. Rev. **120**, 130 (1960).
[6] H. Kettunen, H. Wallén, and A. Sihvola, Proceedings of Metamaterials 2007, Rome, Italy, 22–24 October 2007, pp. 782–785.
[7] H. Wallén, H. Kettunen, and A. Sihvola, Proceedings of Metamaterials 2007, Rome, Italy, 22–24 October 2007, pp. 252–255.
[8] H. Kettunen, H. Wallén, and A. Sihvola, J. Appl. Phys. **102**, 044105 (2007).
[9] *Handbook of Mathematical Functions*, edited by M. Abramowitz and I. A. Stegun (Dover, New York, 1972).
[10] A. A. Sukhorukov, I. V. Shadrivov, and Y. S. Kivshar, Int. J. Numer. Model. **19**, 105 (2006).
[11] L. C. Davis, Phys. Rev. B **14**, 5523 (1976).
[12] M. G. Silveirinha and N. Engheta, Phys. Rev. B **76**, 245109 (2007).
[13] A. Alù and N. Engheta, Plasmonic Resonant Optical Nanoswitch, http://arxiv.org/abs/0710.4895v2 (2007).
[14] J. B. Pendry, Phys. Rev. Lett. **85**, 3966 (2000).
[15] A. Sihvola, *Electromagnetic Mixing Formulas and Applications* (IEE, London, 1999).
[16] D. R. Smith, D. Schurig, M. Rosenbluth, S. Schultz, S. A. Ramakrishna, and J. B. Pendry, Appl. Phys. Lett. **82**, 1506 (2003).
[17] R. Merlin, Appl. Phys. Lett. **84**, 1290 (2004).
[18] V. A. Podolskiy and E. E. Narimanov, Opt. Lett. **30**, 75 (2005).